Available online at www.sciencedirect.com
ScienceDirect
Journal of Power Sources 164 (2007) 386–389
JOURNAL OF POWER SOURCES
www.elsevier.com/locate/jpowsour

Short communication

Electrochemical performance of nanostructured amorphous Co_3Sn_2 intermetallic compound prepared by a solvothermal route

J. Xie *, X.B. Zhao, G.S. Cao, J.P. Tu

Department of Materials Science and Engineering, Zhejiang University, Hangzhou 310027, PR China

Received 7 August 2006; received in revised form 14 August 2006; accepted 16 September 2006
Available online 13 November 2006

Abstract

A nanostructured amorphous Co_3Sn_2 intermetallic compound was prepared by a solvothermal route. The microstructure and the electrochemical performance were studied by X-ray diffraction (XRD), transmission electron microscopy (TEM), galvanostatic cycling, and ex situ XRD. It was found that the as-prepared material is in nanoscale and is amorphous. The amorphous Co_3Sn_2 shows a first specific capacity of 363 mA h g^{-1} compared to 92 mA h g^{-1} for the crystalline one prepared by annealing the amorphous material. Ex situ XRD investigation shows that the amorphous Co_3Sn_2 undergoes a crystallization process during cycling, which leads to the capacity fade.

Keywords: Li-ion batteries; Anode materials; Nanomaterials; Amorphous Co_3Sn_2

1. Introduction

Although carbon-based materials are still the dominant anodes in the commercial Li-ion batteries, in recent years, great interest has been focused on the non-carbonaceous materials with high specific capacity to meet the high-energy density requirement in portable electric devices. Among them, Sn-based materials seem to the suitable candidates due to their high specific capacity (990 mA h g^{-1}) and appropriate Li-storage potential (average 0.5 V versus Li^+/Li). In 1997, Fujiphoto Film Celltec reported that some Sn-based oxides exhibited high specific capacity and stable charge–discharge cycling [1]. To overcome the first irreversible capacity associated with the formation of Li_2O, intermetallic compounds [2–9] instead of oxides are proposed in the following studies. The intermetallic compound is generally composed of Sn and a Li-inactive element such as Fe, Co, Ni, etc. Although the first irreversible capacity can be significantly reduced through the substitution of oxygen ion by transition metals, rapid capacity fade still occurs due to pulverization and exfoliation of the active material caused by the large volume changes upon cycling.

In recent years, tremendous effort has been made to overcome this problem. One is to use materials with a smaller particle size, namely, with a higher surface/thickness ratio. As reported by Yang et al. [10], the cycling stability of intermetallic anodes can be significantly improved by decreasing the particle size to a submicron scale due to the reduced absolute volume changes and enhanced Li-alloying kinetics. When taking above into account, nanomaterials seem to be ideal options because of their extremely large surface/thickness ratios. Previous researches have found that good cycling stability could be achieved in some nanoscaled Sn-based intermetallic compounds [11–13]. More recently, Sakai group [14,15] reported that nanostructured Ag–Fe–Sn and Ag–Sb–Sn systems, prepared by high-energy ball milling, exhibited excellent cycling behavior with a capacity of about 400 mA h g^{-1} retained up to 300 charge and discharge cycles.

Another one is to use amorphous materials instead of crystalline ones. The researches on some amorphous materials showed that these materials generally exhibited good electrochemical performance [16–20]. However, these materials are all in thin-film state prepared by conversional thin-film preparation methods such as chemical vapor deposition (CVD), combinatorial magnetron sputtering, and pulsed laser deposition (PLD), etc. In this work, we will report the electrochemical performance of a nanostructured amorphous intermetallic compound Co_3Sn_2 prepared by a soft chemical method, namely, solvothermal route.

* Corresponding author. Tel.: +86 57 185 662 587; fax: +86 57 187 951 672.
E-mail address: xiejian1977@zju.edu.cn (J. Xie).

0378-7753/$ – see front matter © 2006 Elsevier B.V. All rights reserved.
doi:10.1016/j.jpowsour.2006.09.094

For comparison, the electrochemical performance of the crystalline one will also be reported.

2. Experimental

A nanostructured amorphous Co_3Sn_2 were prepared by the solvothermal route. Analytically pure $CoCl_2{\cdot}6H_2O$ and $SnCl_2{\cdot}2H_2O$ were used as the precursors in the solvothermal synthesis. The precursors in stoichiometric ratio of Co:Sn were put into a Teflon-lined autoclave. The autoclave was then filled with ethanol up to 85% of its volume. After adding sufficient $NaBH_4$ as the reductant, the autoclave was sealed immediately and heated to 220 °C for the synthesis reactions. After reaction for 24 h, the autoclave was cooled down to room temperature naturally. The obtained precipitate was filtered, washed with ethanol and distilled water several times, and dried under vacuum at 110 °C for 12 h. The amorphous Co_3Sn_2 sample was further annealed at 500 °C for 2 h in flowing N_2 to obtain crystalline Co_3Sn_2.

The powders were analyzed by X-ray diffraction (XRD) using a Rigaku-D/MAX-2550PC diffractometer equipped with Cu Kα radiation (λ = 1.5406 Å) in the range of $2\theta = 10$–$80°$. Ex situ XRD was performed on the Co_3Sn_2 electrode to investigate the phase transition during the charge and discharge cycling. The powder morphology was observed on a JEM-2110 transmission electron microscopy (TEM) and field emission scanning electron microscopy (FESEM) on a FEI-Sirion microscopy.

The electrochemical reactions of Co_3Sn_2 with lithium were investigated using a simple two-electrode coin-type cell: Li/$LiPF_6$ (EC + DMC)/Co_3Sn_2. The working electrode consists of 80 wt.% Co_3Sn_2 powder, 10 wt.% acetylene black as conducting agent, 10 wt.% polyvinylidene fluoride (PVDF) as binder, and Ni foam as the substrate (current collector). The cells were assembled in an Ar-filled glove box using polypropylene (PP) micro-porous film as separator, a solution of 1 M $LiPF_6$ in ethylene carbonate (EC)/dimethyl carbonate (DMC) (1:1, v/v) as electrolyte and metallic lithium foil as counter electrode. The cells are charged and discharged at a current density of 20 mA g^{-1} between 0.05 and 1.5 V versus Li^+/Li.

3. Results and discussion

Fig. 1 shows the XRD patterns of Co_3Sn_2 intermetallic compound before and after annealing. Note that only amorphous Co_3Sn_2 is obtained during the solvothermal reactions as seen in Fig. 1(a). After annealing at 500 °C for 2 h, well-crystallized Co_3Sn_2 is formed as shown in Fig. 1(b). The diffraction peaks of the annealed product agree well with the hexagonal Co_3Sn_2 phase with a space group $P6_3/mmc$. The calculated cell parameters are $a = 4.108(7)$ Å, $c = 5.178(3)$ Å, which are in good consistent with the standard values of $a = 4.109$ Å, $c = 5.180$ Å (JCPDS File 27–1124).

Fig. 2 shows the TEM images and electron diffraction (ED) patterns of Co_3Sn_2 intermetallic compound before and after annealing. The diffuse rings in the inset of Fig. 2(a) further prove that the as-prepared Co_3Sn_2 is in an amorphous state. As indicated in Fig. 2(a), the Co_3Sn_2 powder before annealing is composed of irregular granules with a size below 60 nm and the granules are connected one another to form a network structure. Fig. 3(a) clearly shows the network structure. In addition, the Co_3Sn_2 granules are loosely stacked and a multi-porous structure is formed. After annealing, the irregular granules are transformed into a crystalline ball-like structure as shown in Fig. 2(b). However, no obvious crystal growth occurs during annealing. Note that the ball-like granules tend to form aggregation as seen in Fig. 3(b).

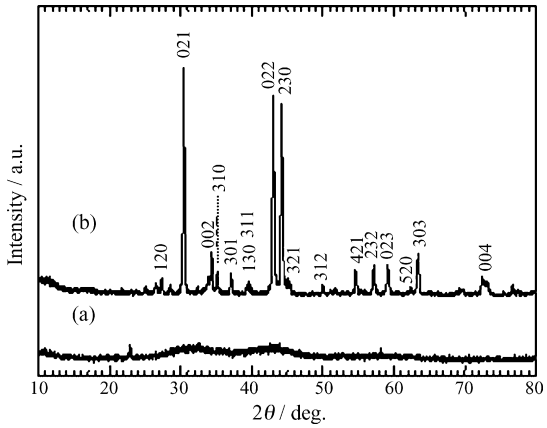

Fig. 1. XRD patterns of the Co_3Sn_2 intermetallic compound: (a) before and (b) after annealing.

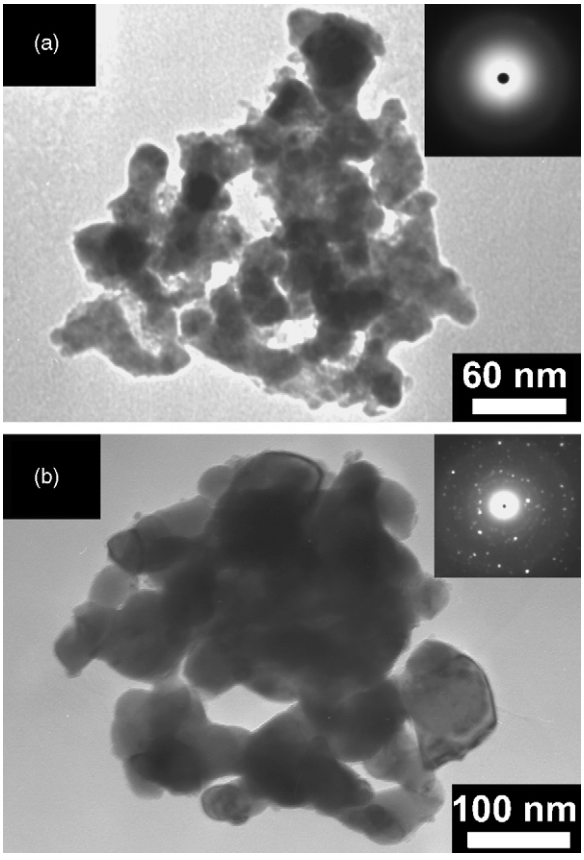

Fig. 2. TEM images and ED patterns of the Co_3Sn_2 intermetallic compound: (a) before and (b) after annealing.

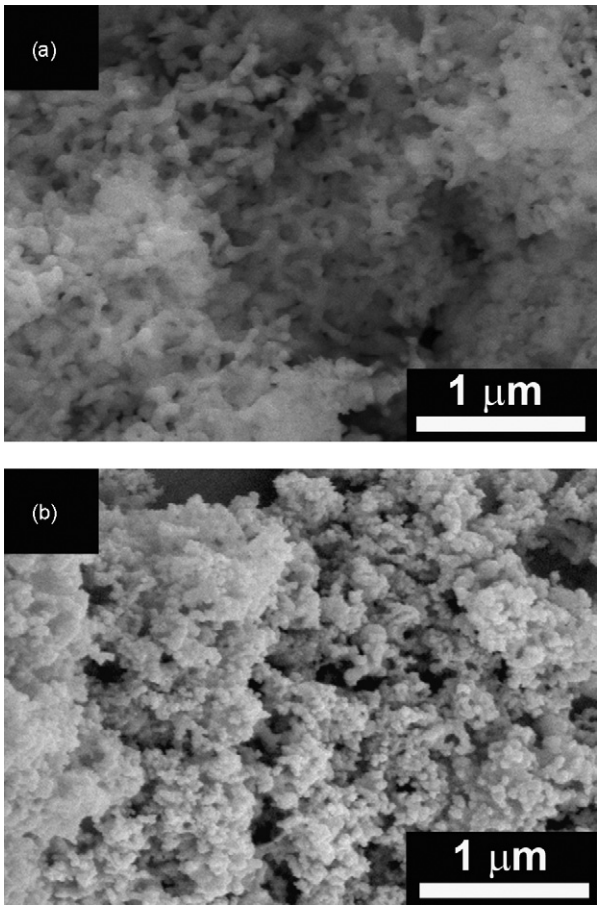

Fig. 3. SEM images of the Co_3Sn_2 intermetallic compound: (a) before and (b) after annealing.

Fig. 4 compares charge and discharge curves between amorphous and crystalline Co_3Sn_2 for the first three cycles. The crystalline Co_3Sn_2 gives a first charge (delithiation) capacity of only 92 mA h g^{-1}, far below its theoretical capacity of 569 mA h g^{-1} (normalized to Co_3Sn_2 per gram) corresponding to the formation of $Li_{4.4}Sn$ composition. This means that crystalline Co_3Sn_2 is electrochemically inactive toward lithium. Recently, Dahn et al. [21] also found that crystalline Co_3Sn_2 is a Li-inactive intermetallic compound even in a thin-film state.

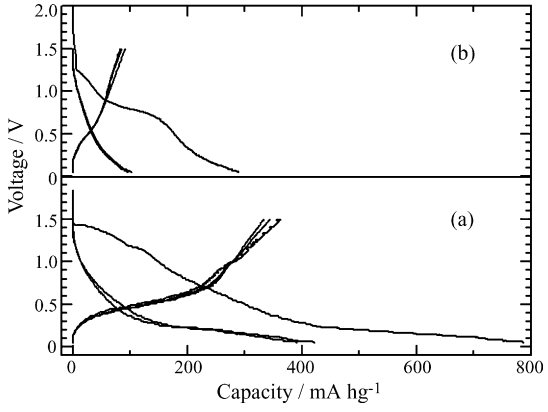

Fig. 4. Charge and discharge curves of (a) amorphous and (b) crystalline Co_3Sn_2 for the first three cycles.

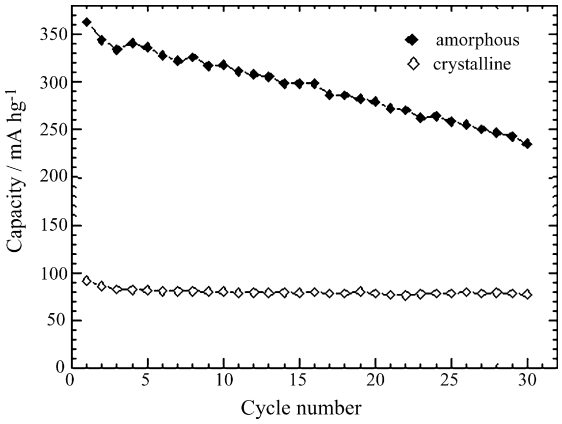

Fig. 5. Comparison of cycling stability between amorphous and crystalline Co_3Sn_2 intermetallic compound.

In contrast, amorphous Co_3Sn_2 yields a first charge capacity of 363 mA h g^{-1}. Although the first charge capacity of amorphous Co_3Sn_2 is still lower than that of its theoretical value, namely, 569 mA h g^{-1}, it is greatly higher than that of its crystalline counterpart. In our opinion, the different electrochemical behaviors between the amorphous and crystalline Co_3Sn_2 can be attributed to their different microstructures since they have the identical chemical composition. For the crystalline Co_3Sn_2, the surface of the active component may be covered with a layer of dense inactive film, just like the Fe "skin" in the $SnFe_3C$ composite [4], which blocks the Li-ion diffusion path. However, the exact structure and composition of the inactive film is unknown so far. For the amorphous one, the inactive film may be rather thin or inexistent. As a result, Li-ions can easily diffuse into the interior of the amorphous granules. In addition, the loose stacking of the granules and the multi-porous structure facilitate the penetration of the electrolyte and Li-ion diffusion.

Fig. 5 compares the cycling stability of amorphous and crystalline Co_3Sn_2. Compared to amorphous Co_3Sn_2, crystalline Co_3Sn_2 exhibits better cycling stability due to the fact that only a small amount of Co_3Sn_2 participates in the electrochemical reactions, and the unreacted Co_3Sn_2 can act as matrix to buffer the volume changes upon cycling. For amorphous Co_3Sn_2, however, the proportion of Co_3Sn_2 acting as the buffer is much

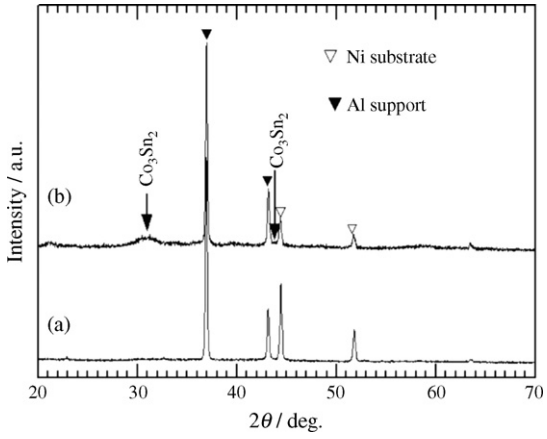

Fig. 6. XRD patterns of amorphous electrodes (a) before and (b) after cycling.

smaller than that of the crystalline one. More importantly, electrochemically generated crystallization takes place upon cycling as indicated in Fig. 6. The crystallization of amorphous Co_3Sn_2 makes it electrochemically inactive toward Li, which results in the continuous capacity fade during the charge and discharge cycling. As a result, for the practical application of this amorphous material in the secondary Li-ion batteries, its microstructure and composition should be further optimized to restrain the crystallization during the charge and discharge cycling and to reduce the first irreversible capacity.

4. Conclusions

Amorphous Co_3Sn_2 can be synthesized by a low-temperature solvothermal route and it shows greatly increased specific capacity than its crystalline counterpart. The improved electrochemical activity of amorphous Co_3Sn_2 is attributed to the lack of the dense inactive film and the loose stacking of the particles. The relatively rapid capacity fade of amorphous Co_3Sn_2 compared to the crystalline one can be attributed to its low buffer matrix amount and the crystallization of the active component upon cycling.

Acknowledgements

The work is supported by National Natural Science Foundation of China (No. 50201014), by Doctoral Program for High Education of China (No. 20010335045), and by China Postdoctoral Science Foundation (No. 2005038278).

References

[1] Y. Idota, T. Kobota, A. Matsufuji, Y. Maekawa, T. Miyasaka, Science 276 (1997) 1395.
[2] O. Mao, R.A. Dunlap, J.R. Dahn, J. Electrochem. Soc. 146 (1999) 405.
[3] O. Mao, J.R. Dahn, J. Electrochem. Soc. 146 (1999) 414.
[4] O. Mao, J.R. Dahn, J. Electrochem. Soc. 146 (1999) 423.
[5] D. Larcher, L.Y. Beaulieu, O. Mao, A.E. George, J.R. Dahn, J. Electrochem. Soc. 147 (2000) 1703.
[6] J.T. Vaughey, K.D. Kepler, R. Benedek, M.M. Thackeray, Electrochem. Commun. 1 (1999) 517.
[7] L. Fransson, E. Nordström, E. Edström, L. Häggström, J.T. Vaughey, M.M. Thackeray, J. Electrochem. Soc. 149 (2002) A736.
[8] K.D. Kepler, J.T. Vaughey, M.M. Thackeray, J. Power Sources 81–82 (1999) 383.
[9] H. Kim, Y.J. Kim, D.G. Kim, H.J. Sohn, T. Kang, Solid State Ionics 144 (2001) 41.
[10] J. Yang, Y. Takada, N. Imanishi, O. Yamamoto, J. Electrochem. Soc. 146 (1999) 4009.
[11] J. Wolfenstine, S. Campos, D. Foster, J. Read, W.K. Behl, J. Power Sources 109 (2002) 230.
[12] H.Y. Lee, S.W. Jang, S.M. Lee, S.J. Lee, H.K. Baik, J. Power Sources 112 (2002) 8.
[13] H. Li, G.Y. Zhu, X.J. Huang, L.Q. Chen, J. Mater. Chem. 10 (2000) 693.
[14] J.T. Yin, M. Wada, S. Tanase, T. Sakai, J. Electrochem. Soc. 151 (2004) A583.
[15] E. Rönnebro, J.T. Yin, A. Kitano, M. Wada, S. Tanase, T. Sakai, J. Electrochem. Soc. 152 (2005) A152.
[16] H. Jung, M. Park, Y.G. Yoon, G.B. Kim, S.K. Joo, J. Power Sources 115 (2003) 346.
[17] L.Y. Beaulieu, K.C. Hewitt, R.L. Turner, A. Bonakdarpour, A.A. Abdo, L. Christensen, K.W. Eberman, L.J. Krause, J.R. Dahn, J. Electrochem. Soc. 150 (2003) A149.
[18] S.W. Song, K.A. Striebel, X.Y. Song, E.J. Cairns, J. Power Sources 119–121 (2003) 110.
[19] M.D. Fleischauer, M.N. Abrovac, J.R. Dahn, J. Electrochem. Soc. 153 (2006) A1201.
[20] J.R. Dahn, R.E. Mar, M.D. Fleischauer, M.N. Abrovac, J. Electrochem. Soc. 153 (2006) A1211.
[21] J.R. Dahn, R.E. Mar, A. Abouzeid, J. Electrochem. Soc. 153 (2006) A361.